An MO−VB Approach for the Determination of Intermolecular Forces. Theory and Calculations on the He_2, $He-CH_4$, and $He-H_2O$ Systems

Gabriele Calderoni, Fausto Cargnoni,* Antonino Famulari, and Mario Raimondi

Dipartimento di Chimica Fisica ed Elettrochimica and Istituto CNR−ISTM, Università degli Studi di Milano, via Golgi 19 -20133 Milano, Italy

Received: March 12, 2002; In Final Form: April 8, 2002

We present the improvement of a previously developed strategy for the evaluation of intermolecular forces. The approach defines a variational VB (valence bond) wave function, consisting of single and double excitations from the SCF-MI (self-consistent field for molecular interactions) determinant. The central idea of the method is the determination of optimal virtual orbitals, to contract the virtual space spanned by all singly and doubly excited localized configurations, by means of an iterative optimization procedure. The performance of the strategy is tested by comparison with results where the full virtual space is considered, and the entire approach is also compared with more conventional quantum chemical methods. Test calculations on three weakly interacting complexes, namely, He_2, $He-CH_4$, and $He-H_2O$, are presented. Whatever the system studied, we found an overall agreement between VB, MP4, and CCSD(T) results. The VB well depths estimates are somewhat larger than MP4 and CCSD(T) ones.

Introduction

Among the difficulties connected with the determination of intermolecular interactions by means of the supermolecular approach, the basis set superposition error (BSSE) represents a well-known inconvenience.[1] To avoid BSSE, two strategies can be followed. A first approach consists of making the monomer description consistent with that of the dimer, adopting a dimer centered basis set (DCBS); in the other approach, based on a monomer centered basis set (MCBS) scheme, the dimer description is made consistent with that of the monomer.[2]

During the years, the computational quantum chemical methods that make use of a DCBS description have received the major interest, and the counterpoise correction[3] has been therefore commonly adopted to evaluate interaction energies. Among the reasons for this choice, we mention the difficulties to efficiently deal with the nonorthogonality, that naturally arises when a MCBS description is considered. Notwithstanding the great popularity received by the counterpoise method, there are some inconveniences associated with it. From a practical viewpoint, the need to calculate the energy of the isolated fragment in the DCBS framework leads to the tedious "3:1 rule" (i.e., three energy calculations for *every* interaction energy to be evaluated),[3] with the situation getting worse if geometric relaxation is taken into account.[4] On the theoretical side, the upsetting of the multipole moments and polarizabilities of the monomers (secondary BSSE) was reported.[5]

Over the past few years, we developed nonorthogonal approaches to the determination of intermolecular interactions.[6−9] Common to them is the partitioning of the global basis set into subsets centered on the interacting subsystems; the molecular orbitals of different fragments are then expanded only in their specific set, in the spirit of the MCBS approach. Because of this partitioning, orbitals belonging to different fragments are nonorthogonal and overlap, reflecting the physics of the problem; in this way, BSSE is naturally avoided in a priori fashion.

* To whom correspondence should be addressed. E-mail: fausto.cargnoni@istm.cnr.it.

The first step was the formulation of the SCF-MI (self-consistent field for molecular interactions) algorithm,[6] which has been successfully adopted in many investigations.[7] Later, we included electron correlation effects by means of a nonorthogonal configuration interaction scheme (MO−VB).[8,9] Similarly to the ICF1 method proposed by Liu and McLean,[10] the essence of the MO−VB scheme is the evaluation of the intermolecular part of the correlation energy only. In this paper, we present a more rigorous formulation of the approach, along with test calculations on three weakly bound complexes. To check the performances of this scheme, we carried out a thorough comparison with more standard Møller−Plesset and coupled cluster DCBS calculations.

The paper is organized as follows. First, the theoretical framework of our approach is described and discussed. Examples of applications to the He_2, $He-CH_4$, and $He-H_2O$ systems are then presented. A final commentary section concludes.

Theory

Build-Up of the Wave Function. Consistent with the MCBS approach, given the interacting system AB (fragments A and B containing N_A and N_B electrons, respectively), the global basis set is partitioned into two subsets belonging to the isolated monomers: each set contains only the basis functions centered on the atoms of its fragment. Starting from the reference SCF-MI[6] wave function, to avoid BSSE, the full CI expansion is assumed in the form

$$[0_A \oplus S_A \oplus D_A \oplus \cdots \oplus N_A] \otimes [0_B \oplus S_B \oplus D_B \oplus \cdots \oplus N_B] \quad (1)$$

where $0_{A/B}$ stands for the reference state and $S_{A/B}$, $D_{A/B}$, ... $N_{A/B}$ represent singly, doubly, ..., *N*-uply excited configurations localized on fragment A or B, respectively. The symbol $\otimes$ represents the direct product of the subspaces; in the context of Grassman or exterior algebra formalism, it is the exterior product

10.1021/jp020681f CCC: $22.00
Published on Web 05/07/2002

of the algebra which includes the antisymmetrization of the global product wave function.

Truncation of expression 1 to any order preserves size consistency. The first-order terms of expansion 1[9] correspond to the following wave function:

$$\Psi_{AB} = C_0\Psi^0_{AB} + \sum_{\substack{a\in \mathrm{occ}A \\ a^*\in \mathrm{virt}A}} C_a^{a^*}\Psi_a^{a^*} + \sum_{\substack{b\in \mathrm{occ}B \\ b^*\in \mathrm{virt}B}} C_b^{b^*}\Psi_b^{b^*} + \sum_{\substack{a\in \mathrm{occ}A \\ b\in \mathrm{occ}B}} \sum_{\substack{a^*\in \mathrm{virt}A \\ b^*\in \mathrm{virt}B}} C_{ab}^{a^*b^*}\Psi_{ab}^{a^*b^*} \quad (2)$$

where Ψ^0_{AB} is the reference SCF-MI wave function, whereas $\Psi_a^{a^*}$ and $\Psi_b^{b^*}$ represent single excitations from the *a* and *b* occupied MOs into the virtual orbitals *a** and *b** of the systems A and B, respectively. $\Psi_{ab}^{a^*b^*}$ are doubly excited configurations resulting from the simultaneous single excitations on both fragments. As the asymptotic limit of expression 2 is considered, the weights of all excited configurations vanish, and the wave function reduces to the SCF-MI term. It is clear that wave function 2, as derived from expression 1, results free of BSSE and appears specifically suited to describe intermolecular dispersion terms.

When the whole spin space is considered, the number of structures N_{struct} partaking to expression 2 is given by

$$N_{\mathrm{struct}} = 1 + O_A V_A + O_B V_B + 2O_A O_B V_A V_B \quad (3)$$

where O_A and O_B represent the number of occupied orbitals in the isolated monomers and V_A and V_B are the number of virtuals. When high quality basis sets are adopted, V_A and V_B are much larger than O_A and O_B; thus, N_{struct} nearly scales with the product of the dimensions of the basis functions subsets. As will be described below, we devised a strategy that reduces dramatically the number of structures to include in the final MO−VB wave function, without appreciable loss in accuracy.

Following the procedure described in ref 9, for any MO pair *ab*, it is possible to determine the pair of localized virtuals *a** and *b** that minimizes the variational energy of the wave function:

$$\Psi' = C_0\Psi^0_{AB} + C_1\Psi_{ab}^{a^*b^*} \quad (4)$$

where the whole spin space is taken into account. Given the optimized orbitals *a** and *b**, their orthogonal complement spaces are determined and used to expand a new virtual pair. The whole procedure, when repeated *n* times, generates *n* optimized virtual orbital pairs for each pair *ab* of occupied orbitals.

The energy contribution corresponding to wave function 4 decreases with increasing *n* and reaches negligible values when *saturation* is approached. The optimized virtual spaces localized on A and B and corresponding to excitations from the *ab* occupied pairs are then indicated as opt*a*(*ab*) and opt*b*(*ab*), respectively. As all of the *ab* pairs have been considered, the final wave function of the supersystem AB, expressed in the form of eq 2, is rewritten as

$$\Psi_{AB} = C_0\Psi^0_{AB} + \sum_{\substack{a\in \mathrm{occ}A \\ a^*\in \mathrm{opt}a(ab)}} C_a^{a^*}\Psi_a^{a^*} + \sum_{\substack{b\in \mathrm{occ}B \\ b^*\in \mathrm{opt}b(ab)}} C_b^{b^*}\Psi_b^{b^*} + \sum_{\substack{a\in \mathrm{occ}A \\ b\in \mathrm{occ}B}} \sum_{\substack{a^*\in \mathrm{opt}a(ab) \\ b^*\in \mathrm{opt}b(ab)}} C_{ab}^{a^*b^*}\Psi_{ab}^{a^*b^*} \quad (5)$$

where excitations from any pair *ab* of occupied orbitals are thus restricted to the corresponding optimal virtual spaces. Wave function 5 gives results nearly equivalent to the *full* wave function, as given in 2, despite the decrease in the number of configurations. In both cases, the energy is calculated by solving the proper secular problem by means of standard VB techniques.[11]

The iteration of eq 4 up to *saturation* of dispersion energy contributions is therefore the true novelty of the present approach. As it will be shown in the next paragraphs, usually few virtual orbital pairs for each MO couple account for most of the correlation energy, and this feature is nearly independent of the basis set adopted. This implies that the number of configurations to be included in the final wave function is efficiently reduced, and it depends only on the molecular system considered, and more importantly, it does not increase with the basis set size.

Commentary. A key point of the method presented is the adoption of the MCBS scheme to expand the molecular complex wave function. Theoretically, this approach does not preclude the possibility to reach the complete basis set limit, for both the interacting fragments and the complex. As finite basis set calculations are considered, the MCBS and DCBS orbital descriptions may differ significantly, especially when small basis sets are adopted and significant electron density rearrangements between the interacting fragments are present.[2,12,13,15] In these situations, the limits imposed to the orbital expansion within the MCBS scheme could appear too severe and usually result in the underestimate of the complex interaction energy[12] and monomer deformation contributions.[13] Indeed, the opposite is true when a DCBS expansion is considered, as reviewed by Chalasinski and Szczesniak.[13] When basis sets with increasing size are adopted, the MCBS and DCBS descriptions significantly approach one another, as shown in the case of the water dimer.[7] In fact, the study of the Hartree−Fock limit properties of this system showed good agreement between the best SCF-MI estimate of the interaction energy (−5.50 mE_h), obtained with a total of 338 basis set functions,[7] and SCF calculations (−5.80 mE_h) carried out with a definitely larger basis set of over a thousand basis functions.[14]

Though in general it is possible that DCBS calculations converge to the complete basis set limit somewhat faster,[13,15] the MCBS scheme a priori avoids BSSE, and therefore, it represents a valid candidate for geometry optimization. Our group implemented an analytical procedure within the SCF-MI algorithm.[6] This could be extended to VB calculations of the present form, since Dijkstra and van Lenthe[16, 17] recently provided the analytical expressions for energy first derivatives, even if this is not yet implemented in our codes.

Finally, a comment on the correlation energy estimate performed by our method is mandatory. The fundamental approximation of the present scheme is the truncation of expression 1 to first order. Roughly speaking, this scheme efficiently accounts for the intermolecular interaction energy contribution, but it does not include the intramolecular terms at second and higher orders. Because in van der Waals systems their overall contribution is usually repulsive,[18] our calculations are expected to slightly overestimate the complexes formation energy.

Calculations and Results

In the present section, several examples of application of the new extended MO−VB approach are presented and discussed. The He_2, He−CH_4, and He−H_2O systems have been extensively

TABLE 1: Potential Energy Surface Properties for the Helium Dimer from VB Calculations[a]

level	D_e (μE_h)	r_e (bohr)	σ (bohr)
VB_I	−13.77	6.262	5.458
VB_II	−19.99	5.913	5.271
VB_III	−28.10	5.758	5.114
VB_IV	−28.21	5.754	5.111
VB_V	−28.27	5.754	5.109
VB_VI	−28.29	5.754	5.106
VB_VII	−28.30	5.753	5.103
VB_VIII	−28.34	5.749	5.103
VB_IX	−28.42	5.749	5.103
VB_X	−28.42	5.748	5.102
VB_F	−28.46	5.745	5.101

[a] Well depth D_e, equilibrium distance r_e, and σ are computed employing the aug-cc-pVTZ basis set.

studied. To reach high accuracy and consistency with available experimental and theoretical results, augmented correlation consistent basis sets[19] have been employed. The efficiency of the method has been investigated with respect to both the dimension of the contracted virtual spaces and the basis set quality.

The SCF-MI wave functions were obtained by means of the GAMESS−US suite of programs,[20] whereas MO−VB calculations have been carried out employing modified versions of the codes described in refs 8 and 9. The current implementation of the algorithm allows us to employ a maximum of 255 basis set functions. With regard to the comparison with the standard methods, Møller−Plesset and coupled-cluster calculations were carried out with the GAMESS−US and the Gaussian[21] codes, respectively, applying counterpoise correction.[3]

I. The Helium Dimer. The helium dimer represents the ideal candidate to test the accuracy of ab initio methods concerning weak intermolecular interactions. The quite unique properties of this interaction are indeed well-known and have been the subject of many investigations both on the experimental and on the theoretical side. For a thorough list of ab initio results, we refer the interested readers to the works of Woon et al.,[22] van Mourik et al.,[23,24] and the references therein.

Among the most accurate calculations we mention the Quantum Monte Carlo (QMC) investigations by Anderson et al.[25] who found values of 34.86 ± 0.32 μE_h and 34.77 ± 0.06 μE_h at the internuclear distance of 5.6 bohr. The symmetry adapted perturbation theory (SAPT) approach used by Korona and co-workers with inclusion also of relativistic effects[26] provided a well depth of 35.02 μE_h. Komasa and Rychlewsky[27] found a well depth of 34.68 μE_h at an equilibrium distance of 5.6 bohr, employing explicitly correlated Gaussian functions. Studies employing more standard high level theories are also present in the literature.[22−24,28]

The most accurate general potentials available for the helium dimer are the HFD-B3−FCI1 proposed by Aziz et al.,[29] successively improved by Janzen and Aziz[30] to take account of the SAPT theoretical results of Korona et al.[26]

As concerning our approach, all double excitations assume the form $\Psi_{1,1}^{a^*b^*}$, where (1,1) indicates the single MO occupied pair in this system, whereas a^* and b^* lie in the corresponding opt$a$(1,1) and opt$b$(1,1) virtual spaces. The dimension of the contracted virtual spaces corresponds to the number n of successive optimal virtuals obtained employing wave function 4. In the following, n will be used to label the corresponding final MO−VB wave function 5 as VB_n.

The efficiency of the approach can be deduced by the analysis of data in Table 1 and Figure 1, obtained with the aug-cc-pVTZ basis set. As the level n of the calculation increases, the properties of the interaction potential rapidly converge to the limit, indicated as VB_F, where the full virtual space provided by the SCF-MI calculation is employed. As reported in Table 1, the restriction of opt$a$(1,1) and opt$b$(1,1) to only three virtual pairs is already sufficient to recover a large part of the correlation energy obtained at the VB_F level. More precisely, the well depth, corresponding to the VB_III wave function, reproduces the VB_F limit within 0.5 μE_h, and r_e (the minimum of the well depth) and σ (the distance where the interaction becomes repulsive) are overestimated only by about 0.01 bohr. Moving step by step from the IIIth to the Xth level, we observe a quite regular recovering of the remaining interaction energy, with the same applying for r_e and σ. The VB_X potential reaches complete agreement with the VB_F case, and the two interaction curves are nearly equivalent to each other (see Figure 1). The described features do not vary when other basis sets are adopted: VB_III and VB_X data differ less than 1 μE_h, and the corresponding changes of r_e and σ amount to a very small variation of about 0.01 bohr.

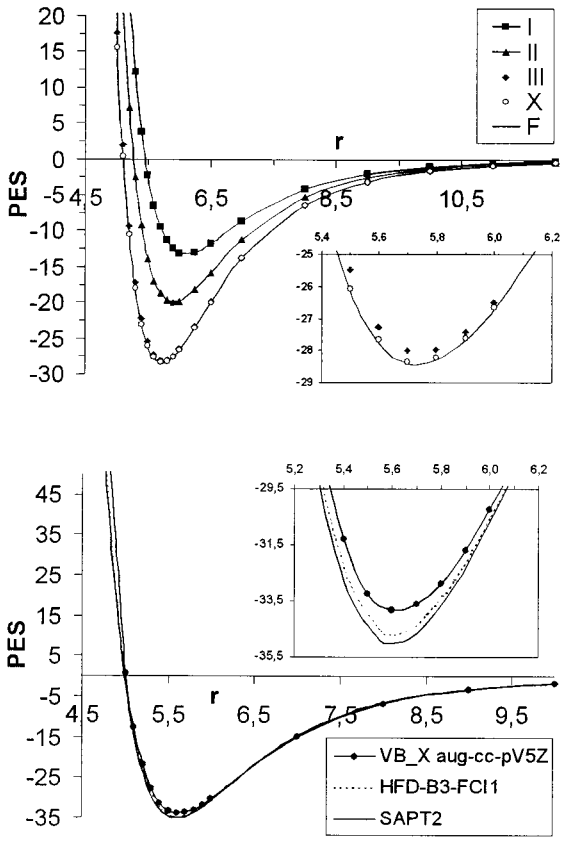

Figure 1. Potential energy surfaces for the helium dimer. Top panel: aug-cc-pVTZ basis set, calculations at different VB levels. Bottom panel: attractive part of the He_2 interaction curve according to the most accurate potentials proposed by Aziz et al.[29] (HFD-B3−FCI1) and by Korona et al. (SAPT)[26] and to our VB_X/aug-cc-pV5Z calculations. Interaction energies are expressed in μE_h, and the internuclear distances are in bohr.

The accuracy of the method is further illustrated by comparing the VB_X potential energy surfaces (PES) with those obtained using more conventional computational techniques, namely, the Møller−Plesset (MPn, n = 2−5), coupled cluster (CCSD, CCSD(T), and CCSDT) and full configuration interaction (FCI) approaches.[22,23] Data obtained with the aug-cc-pVnZ (n = 2−5) basis set series are reported in Table 2.

The analysis of Table 2 clearly indicates that, as outlined by van Mourik et al.,[23] MP2 and MP3 calculations are strongly

TABLE 2: Interaction Energies D_e and Equilibrium Distances r_e for the Helium Dimer: Comparison between Different Methods and Basis Sets[a]

basis set	method	D_e (μE_h)	r_e (bohr)
aug-cc-pVDZ	MP2	−12.69	6.168
	MP3	−16.46	6.057
	MP4	−17.95	6.021
	MP5	−18.64	6.005
	CCSD	−16.78	6.058
	CCSD(T)	−18.56	6.009
	CCSDT	−19.13	5.994
	FCI	−19.14	5.994
	VB_F	−21.79	5.913
aug-cc-pVTZ	MP2	−17.96	5.918
	MP3	−23.75	5.798
	MP4	−26.10	5.760
	MP5	−27.19	5.743
	CCSD	−23.76	5.806
	CCSD(T)	−27.09	5.745
	CCSDT	−27.93	5.732
	FCI	−27.97	5.731
	VB_X	−28.42	5.748
	VB_F	−28.46	5.745
aug-cc-pVQZ[b]	MP2	−19.66	5.861
	MP3	−26.00	5.688
	MP4	−28.53	5.651
	MP5	−29.70	
	CCSD	−25.79	5.703
	CCSD(T)	−29.63	5.636
	CCSDT	−30.52	
	FCI	−30.56	
	VB_X	−31.61	5.695
aug-cc-pV5Z	MP2	−20.70	5.824
	MP3	−27.40	5.707
	MP4	−30.06	5.669
	CCSD	−27.08	5.721
	CCSD(T)	−31.24	5.654
	CCSDT	−32.15	5.641
	VB_X	−33.91	5.647

[a] Apart from VB data, all other values are taken from refs 23 and 22. [b] MP5 D_e value are obtained at the MP4/aug-cc-pVQZ equilibrium distance; CCSDT and FCI D_e data are estimated at the CCSD(T) r_e value.

inadequate to correctly describe the He_2 system. As higher order MP results are considered, the differences with respect to FCI calculations are limited to about 1−2 μE_h in the D_e estimate and to few hundredths of a bohr in the case of r_e. A similar picture applies for coupled cluster calculations. At the CCSD level, the D_e is underestimated by approximately 5 μE_h with respect to the FCI limit; a significantly better agreement is found at the CCSD(T) level, and finally, the CCSDT data, concerning both the interaction energy and the equilibrium distance, are nearly equivalent to the FCI ones.

Contrary to the other methods considered, our approach leads to a slight overestimate of the He_2 interaction energy with respect to the FCI limit. This effect is probably to be ascribed to the truncation of expansion 1 to expression 2. Notwithstanding our approximation level, the evaluation of the helium dimer PES is in good agreement with FCI data: the overestimate of D_e is 2.5 μE_h when the aug-cc-pVDZ basis set is employed (to be compared with the underestimate of 2.3 μE_h obtained at the CCSD(T) level), and it reduces to 0.5 μE_h at the aug-cc-pVTZ level and to about 1 μE_h when the aug-cc-pVQZ set is adopted (the corresponding underestimates at the CCSD(T) level are 0.9 and 1.0 μE_h, respectively).

As the larger basis set is considered, MP2, MP3, MP4, and CCSD D_e values are still far from the current estimate of about 35 μE_h.[26,29] Conversely, the CCSD(T) and CCSDT results (about 31 and 32 μE_h, respectively) are comparable to each other and close to our value of about 34 μE_h.

Concerning the evaluation of the equilibrium distance r_e, the methods that give accurate D_e values (CCSD(T), CCSDT, and VB beyond X level) are in agreement with each other within few hundredths of a bohr. As the aug-cc-pV5Z basis set is considered, CCSD(T), CCSDT, and VB_X r_e data fairly agree lying close to 5.65 bohr, overestimating the best available data[26,29] by about 0.05 bohr.

To further check the accuracy of our results (aug-cc-pV5Z basis set, VB_X calculations), we performed a more detailed comparison with the He_2 interaction potentials proposed by Aziz et al.[29] and Korona et al.,[26] testing also the repulsive part of the curve up to 3.0 bohr (see Figure 1). The relevant features of the PES are reported in Table 3, where we include also the results of a preliminary investigation.[31] As can be seen in Figure 1, the attractive part of the VB_X/aug-cc-pV5Z interaction fits well the HFD-B3−FCI1[29] and SAPT[26] energy curves, with appreciable differences being present only in a very limited region around the equilibrium distance. The agreement with these potentials is confirmed when the repulsive portion of the curve is analyzed. In fact, although the VB_X estimate of r_e is in error for about 0.05 bohr, σ agrees with the HFD-B3−FCI1[29] and SAPT[26] value of 4.99 bohr within 0.01 bohr. More importantly, VB_X calculations reproduce well the repulsive interaction energies from 5.0 up to 3.0 bohr: the error is limited to 3% at 4.5 bohr and further reduces at 4.0 and 3.0 bohr.

The present investigation leads to significant improvements with respect to our previous VB study.[31] The estimate of D_e improves slightly (from 33.77 to 33.91 μE_h), but the error on the equilibrium distance reduces markedly (from about 0.15 to 0.05 bohr), and the previous overestimate of σ by 0.1 bohr is completely corrected. Finally, the interaction energy in the repulsive region of the potential decisively approaches the HFD-B3−FCI1[29] and SAPT[26] values, with the computed differences decreasing from 15−35% to 1−3%.

II. He−H_2O. Complexes of water with rare gases can be viewed as models for the interactions of neutral molecules with water. The Ar−H_2O system, for example, has been the subject of studies by high-resolution experiments and high level ab initio calculations.[32] The He−H_2O system is of considerable importance in interstellar chemistry for its collision dynamics,[33] whose modeling requires accurate potential energy calculations.[34−36] Experimental information on the He−H_2O surface comes from the pressure broadening of the vibrational spectral lines of water[37] and beam scattering experiments.[38]

The evaluation of the entire PES of the He−H_2O system is beyond the scope of the present work. To test the performance of the present approach, we calculated the interaction energy of the complex along four radial paths. As shown in Figure 2, the He−H_2O arrangement is described in terms of polar coordinates, with the origin placed at the water molecule center of mass. According to previous theoretical investigations,[34−36] the path defined by $\theta = 75°$ and $\varphi = 0°$ samples the region of the PES global minimum. To get information onto the PES anisotropy, we sampled three addictional radial trajectories, the helium atom approaching the water molecule along its C_2 symmetry axis, alternatively toward oxygen ($\theta = 0°$; $\varphi = 0°$) and the hydrogens ($\theta = 180°$; $\varphi = 0°$), and a single path out of the water molecule plane ($\theta = 90°$; $\varphi = 90°$) and essentially pointing onto the oxygen atom. The notation adopted to label the different trajectories is reported in Table 5.

The convergence of the VB_*n* method is tested by using the aug-cc-pVDZ basis set and the *global minimum* approach. Data

TABLE 3: He_2 Potential Energy Surfaces: Comparison between VB Results and Best Available Data[a]

	D_e (μE_h)	r_e (bohr)	σ (bohr)	E(4.5) (μE_h)	E(4.0) (μE_h)	E(3.0) (μE_h)
HFD-B3−FCI1[29]	−34.66	5.61	4.99	185.65	933.65	12118.31
SAPT2[30]	−35.02	5.60	4.99	183.75	923.32	11904.03
VB_X/aug-cc-pV5Z	−33.91	5.65	5.00	189.78	939.72	11994.39
ref 31	−33.77	5.77	5.11	252.18	1142.03	13794.50

[a] Columns V−VII: He_2 interaction energy E at the short distances indicated in parentheses.

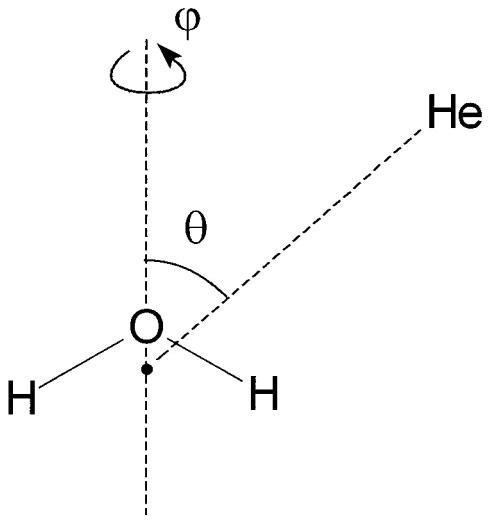

Figure 2. Schematic representation of the He−H_2O complex. Polar coordinates are defined with respect to the water center of mass.

TABLE 4: He−H_2O System: Convergence of VB_*n* Calculations to the VB_F Limit[a]

method	D_e (μE_h)	r_e (bohr)	σ (bohr)
VB_I	−57.5	6.54	5.81
VB_II	−93.3	6.30	5.55
VB_III	−111.9	6.18	5.47
VB_IV	−113.6	6.16	5.46
VB_V	−114.8	6.14	5.45
VB_F	−116.0	6.12	5.44

[a] Interaction energy curve properties along a single radial trajectory (see text for details). All calculations are performed with the aug-cc-pVDZ basis set. D_e is the well depth along the considered trajectory, r_e is the corresponding distance between the helium atoms and the H_2O center of mass, and σ is the distance where the curve becomes repulsive.

obtained from different level VB calculations, up to the VB_F limit (where all virtuals are included in wave function 2), are reported in Table 4 and Figure 3. Similar to the He_2 case, double excitations arising from a given MO pair require at least three virtual orbital pairs to take care of most of the correlation energy, whereas the effect of further virtuals is much smaller. The errors on the r_e and σ values, as compared with the VB_F case, reduce from about 0.15 and 0.25 bohr, respectively, at the VB_I level to few hundredths of a bohr at the VB_III level. The VB_III D_e estimate agrees with the VB_F value within about 5 μE_h. As the two following steps are considered (namely, VB_IV and VB_V data), the PES along the path considered becomes nearly equivalent to the VB_F limit, as shown in Figure 3.

The comparison with global minimum estimates given by conventional quantum mechanical methods (MPn, $n = 2$, 3, and 4; CCSD(T)) was carried out adopting three different basis sets: aug-cc-pVDZ, aug-cc-pVTZ, and aug-cc-pV(Q/T)Z (quadruple for He and triple Z for the H_2O atoms). The results are reported in Table 5 and in Figure 3. Møller−Plesset data significantly vary moving from second to fourth order, and MP4 results fairly agree with the CCSD(T) ones. Taking the helium dimer as a reference, both MP4 and CCSD(T) calculations

TABLE 5: He−H_2O System: Comparison between Different Methods and Basis Sets[a]

basis set	method[b]	D_e (μE_h)	r_e (bohr)	σ (bohr)
Global Minimum Approach ($\theta = 75°$; $\varphi = 0°$)				
aug-cc-pVDZ	MP2	−77.5	6.44	5.67
	MP3	−86.1	6.35	5.60
	MP4	−97.5	6.25	5.53
	CCSD(T)	−98.4	6.24	5.53
	VB_V	−121.2	6.14	5.45
aug-cc-pVTZ	MP2	−104.7	6.12	5.45
	MP3	−120.0	6.06	5.39
	MP4	−136.1	6.02	5.35
	CCSD(T)	−137.0	6.01	5.34
	VB_V	−152.2	5.98	5.31
aug-cc-pV(Q/T)Z	MP2	−113.5	6.18	5.43
	MP3	−128.0	6.12	5.38
	MP4	−143.5	6.08	5.33
	VB_V	−160.4	6.05	5.29
aug-cc-pVQZ	MP2	−118.0	6.16	5.41
	MP3	−133.0	6.10	5.36
	MP4	−149.0	6.06	5.31
Hydrogens Approach ($\theta = 180°$; $\varphi = 0°$)				
aug-cc-pVTZ	MP4	−82.2	6.65	5.90
	CCSD(T)	−88.7	6.60	5.84
	VB_V	−103.9	6.48	5.72
Oxygen Approach ($\theta = 0°$; $\varphi = 0°$)				
aug-cc-pVTZ	MP4	−81.2	6.44	5.70
	CCSD(T)	−83.8	6.41	5.67
	VB_V	−102.9	6.31	5.52
On Top Approach ($\theta = 90°$; $\varphi = 90°$)				
aug-cc-pVTZ	MP4	−48.5	6.91	6.15
	CCSD(T)	−52.7	6.87	6.08
	VB_V	−64.8	6.69	5.91

[a] Interaction energy curves along three different radial trajectories (see text for details). [b] Counterpoise correction applied in all cases, with the exception of VB_V data.

should slightly underestimate the well depth with respect to FCI results. Whatever the basis set adopted, our calculations give a more attractive potential (about 15 μE_h) with respect to these methods. The MP4, CCSD(T), and VB_V estimates of r_e and σ generally agree within few hundredths of a bohr, and the accordance improves as larger basis sets are considered. On the contrary, MP2 and MP3 data markedly differ with respect to the above-mentioned calculations. The extent of the counterpoise correction in the region of the global minimum ($r = 6.00$ bohr) is about 90 μE_h at the MP4/aug-cc-pVDZ level and reduces significantly when larger sets are adopted (MP4/aug-cc-pVTZ, 27 μE_h; MP4/aug-cc-pVQZ, 14 μE_h). The same trend is found for CCSD(T) results.

The VB_V/aug-cc-pV(Q/T)Z data indicate a minimum interaction energy close to 160 μE_h at the distance of 6.05 bohr. These results compare well with our MP4/aug-cc-pVQZ data and with the estimates extracted from MP4,[35] SAPT/MP4,[39] and scaled perturbation theory[36] investigations.

As concerns the other trajectories considered, the local minima obtained along the *hydrogens* and *oxygen* approaches (VB_V/aug-cc-pVTZ calculations) are nearly degenerate in energy and result about 50 μE_h higher with respect to the *global minimum*. In the *oxygen* approach, r_e and σ are respectively 0.3

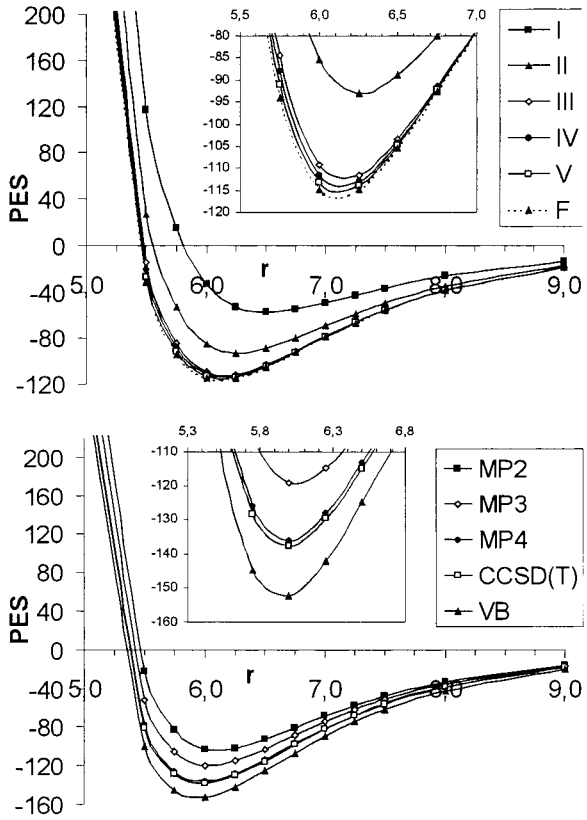

Figure 3. Interaction energy curve for the He−H_2O system along the global minimum approach. Top panel: convergence of VB_*n* (n = 2−5) calculations to the VB_F limit using the aug-cc-pVDZ basis set. Bottom panel: comparison between VB data and other theoretical methods (aug-cc-pVTZ basis set). The distance r between helium and the H_2O center of mass is expressed in bohr. Interaction energies are in μE_h.

and 0.2 bohr larger than in the *global minimum* case, and these values nearly double as the *hydrogens* approach is considered. An analogous behavior is obtained at MP4 and CCSD(T) level. The main difference between the three methods is the larger energy estimate of the local minima given by VB calculations (about 20 μE_h). Similar considerations apply to the *on top* approach: whatever the method considered, the well depth locates about 90 μE_h higher in energy with respect to the *global minimum*, whereas r_e and σ are about 0.75 and 0.6−0.8 bohr, respectively, larger than in the absolute minimum case. Finally, VB_V/aug-cc-pVTZ data are in good agreement with the PES recently calculated by Hodges et al.[36] These authors proposed a global minimum well depth of 159.2 μE_h at $r_e = 5.90$ bohr ($\theta = 78.3°$, $\varphi = 0.0°$); the *oxygen* and *hydrogens* local minima are nearly degenerate ($D_e = -96.7$ and -98.7 μE_h) and locate at 6.19 and 6.66 bohr, respectively.

An overall comparison of the data calculated with the aug-cc-pVTZ basis set, and reported in Table 5, suggests that MP4, CCSD(T), and VB calculations would probably recover the same He−H_2O PES topology. Though the VB interaction energies are systematically larger than the MP4 and CCSD(T) ones, the D_e values of the local minima along the four analyzed radial trajectories are predicted in the same order by the various methods adopted. The discrepancies in the estimates of r_e and σ between VB and the two other methods are limited to 0.05 bohr when the *global minimum* approach is considered and, as expected, become somewhat larger (0.15 bohr) when the other, less attractive, trajectories are considered.

TABLE 6: He−CH_4 System Face Approach: Convergence of VB_*n* Calculations to the VB_F Limit[a]

method	D_e (μE_h)	r_e (bohr)	σ (bohr)
VB_I	−53.9	7.03	6.25
VB_II	−95.6	6.71	5.94
VB_III	−129.2	6.54	5.78
VB_IV	−134.3	6.49	5.73
VB_V	−135.6	6.49	5.73
VB_F	−137.4	6.47	5.71

[a] Interaction energy curve properties along the face approach trajectory (see text for details). All calculations performed with the aug-cc-pVDZ basis set.

III. He−CH_4. The study of the complexes of methane with rare gases received great interest in the last years, and several experimental studies are available in the literature.[40,41] Because most of the physical properties of these complexes depend on the features of potential energy surface, its accurate determination has been the subject of many theoretical studies. Similar to the helium dimer system, the He−CH_4 complex is stabilized mainly by dispersion forces. Buck et al.[40] proposed a semiempirical PES, obtained by fitting data from crossed beam experiments and RHF calculations. On the theoretical side, several ab initio PES were recently proposed.[9,42,43] The estimates of the global minimum well depth range from 80 to 125 μE_h.

According to literature results,[9,40,42,43] the absolute minimum of the complex PES corresponds to a *face* arrangement, where the He atom approaches methane along a C_3 axis and points toward carbon. We therefore selected the *face* radial path and the aug-cc-pVDZ basis set to estimate the convergence of the VB approach to the *full* limit. Depending on the method adopted (VB or MP4), we tested basis sets up to the aug-cc-pVQZ level. To evaluate the PES anisotropy, we carried out MP4 and VB calculations (aug-cc-pVTZ basis set) along the radial trajectories usually referred to as *vertex* (He pointing toward hydrogen along a C_3 axis) and *edge* (He approaching the molecule along a C_2 axis) arrangements.

Analogous to the previously described systems, the saturation of the correlation energy (see Table 6 and Figure 4) is substantially reached at the VB_III level, and further steps give definitely minor contributions. The VB_V/aug-cc-pVDZ potential energy surface along the *face* approach is nearly equivalent to the VB_F limit. More precisely, the VB_III estimate of the global minimum D_e still lacks about 8 μE_h with respect to the VB_F case, whereas r_e and σ are overestimated by approximately 0.07 bohr. As VB_V results are considered, the D_e error is reduced to 2 μE_h, whereas r_e and σ agree with the VB_F data within 0.03 bohr.

Whatever the basis set adopted, the VB_V interaction energy estimate is larger than MP4 and CCSD(T) data (see Table 7). At the aug-cc-pVDZ level, for example, MPn data converge toward a D_e value of about 95 μE_h. Slightly larger values are found at CCSD(T) level, whereas the VB_V estimate reaches about 135 μE_h. Consistent with this effect, the r_e and σ values found at VB_V level are about 0.25 bohr smaller than MP4 and CCSD(T) data.

When the aug-cc-pVTZ basis set is taken into account, these effects are substantially maintained, apart for a slightly closer agreement between VB_V and MP4 calculations on the estimates of r_e and σ. The minimum interaction energy is 116.1 μE_h at MP4 level, whereas the VB_V prediction is 157.3 μE_h, to be compared with the experimental value of 123.0 μE_h.[40] The VB_V equilibrium distance r_e (6.35 bohr) finely agrees with the experimental value of 6.4 bohr, whereas the MP4 result is somewhat overestimated (6.54 bohr).

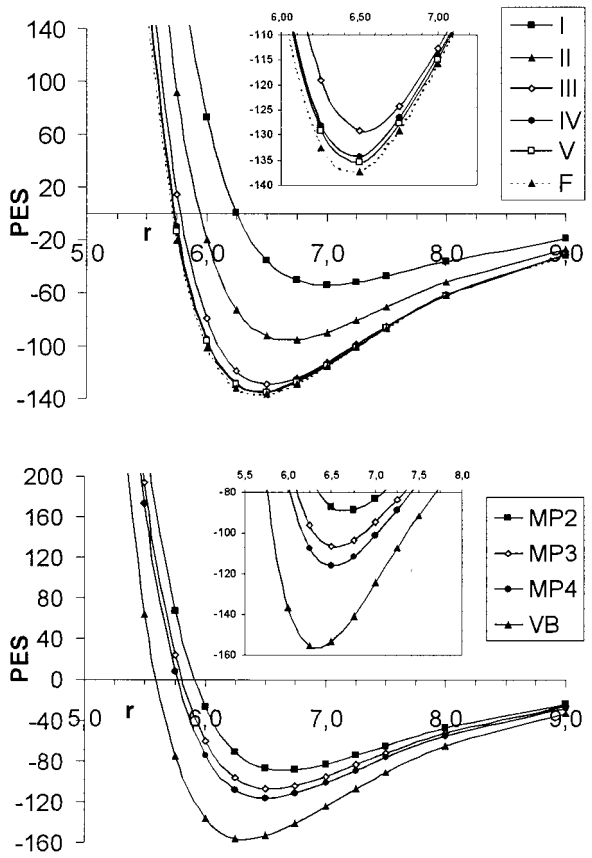

Figure 4. Interaction energy curve for the He−CH_4 system along the face approach. Top panel: convergence of VB_*n* ($n = 2-5$) calculations to the VB_F limit using the aug-cc-pVDZ basis set. Bottom panel: comparison between best VB data and other theoretical methods (aug-cc-pVTZ basis set). The distance *r* between helium and carbon is expressed in bohr. Interaction energies are in μE_h.

When the aug-cc-pVQZ basis set is adopted, the lowering of the minimum interaction energy is quite limited (about 10 μE_h), and the equilibrium distance slightly shortens (see Table 7, MP4 data). The extent of the counterpoise correction in the proximity of the minimum ($r = 6.50$ bohr) decreases from 135 μE_h in the case of MP4/aug-cc-pVDZ results to about 44 μE_h when the MP4/aug-cc-pVTZ data are considered. The correction further reduces to 12 μE_h when the larger aug-cc-pVQZ basis set is adopted.

The agreement between MP4 and VB_V results along the *vertex* and *edge* trajectories significantly increases with respect to the *face* approach. Notwithstanding the fact that VB_V energy profiles are always more attractive than the MP4 ones, the differences between the local well depths estimates are reduced to about 15−20 μE_h, whereas r_e and σ data agrees to within 0.10 bohr (see Table 7). The VB_V/aug-cc-pVTZ calculated interaction energies and equilibrium distances for these approaches finely fit the PES of Buck et al.

Finally, data in Table 7 indicate that the differences between experimental[40] and calculated interaction energies for the He−CH_4 complex are mainly due to the larger He−CH_4 PES anisotropy recovered by VB and MP4 calculations with respect to experimental data.

Concluding Remarks

In the present paper, we have proposed an improved MO−VB computational approach to deal with the determination of intermolecular forces. The method, size consistent and free from BSSE, provides a wave function that is compact and easy to interpret on physical terms even when extended basis sets are employed. The work here detailed represents the improvement of a previously developed strategy.[9] A nonorthogonal localized configuration interaction wave function is adopted. The central idea of the approach is the contraction of the SCF-MI virtual space spanned by singly and doubly excited localized configurations by means of an iterative optimization procedure. As extensively shown, few optimal virtual orbitals are required to recover most of the correlation contributions. The capability of high quality basis sets are thus fully exploited, still requiring a reduced number of structures in the MO−VB wave function. This represent a key point from a computational point of view and is the true novelty of the present scheme with respect to previous VB calculations.[9] With regard to this point, it is to be noted that the number of structures to be inserted in the global MO−VB wave function is almost independent of the dimension of the basis set.

The approach here presented has been tested on three weakly interacting systems, namely, the He_2, He−CH_4, and He−H_2O complexes. The number of configurations for the VB_V wave function varies from 36 in the case of He_2 to 126 for the other systems.

For the He_2 system, the MO−VB results compare well with high level ab initio calculations such as CCSD(T), CCSDT, and MP5. Comparison with the HFD-B3−FCI1 and SAPT potentials shows satisfactory agreement both in the region of the well depth and at the short repulsive distances. With regard to the He−H_2O complex, the results are in accordance with MP4 and CCSD(T) calculations and compare favorably with current theoretical estimates. The PES anisotropy evaluated with our VB scheme is less marked than are the CCSD(T) and MP4 ones.

TABLE 7: He−CH_4 System: Comparison between Different Methods and Basis Sets[a]

basis set	method[b]	D_e (μE_h)	r_e (bohr)	σ (bohr)
	Face Approach			
aug-cc-pVDZ	MP2	−69.3	6.94	6.10
	MP3	−81.6	6.78	5.99
	MP4	−95.7	6.74	5.96
	CCSD(T)	−97.5	6.73	5.95
	VB_V	−135.6	6.49	5.73
aug-cc-pVTZ	MP2	−88.7	6.68	5.91
	MP3	−107.1	6.57	5.80
	MP4	−116.1	6.54	5.77
	VB_V	−157.3	6.35	5.60
aug-cc-pVQZ	MP2	−110.8	6.61	5.85
	MP3	−118.5	6.52	5.75
	MP4	−124.8	6.47	5.72
	VB[9]	−76.5	6.77	5.99
	MP2[42]	−90.7	6.67	5.91
	MP4[42]	−121.2	6.54	5.76
	MP3[43]	−87.0	6.61	
	expt[40]	−123.0	6.4	
	Vertex Approach			
aug-cc-pVTZ	MP2	−46.1	7.95	7.17
	MP3	−59.4	7.80	7.02
	MP4	−64.4	7.76	6.98
	VB_V	−77.4	7.68	6.91
	expt[40]	−65.6	7.7	
	Edge Approach			
aug-cc-pVTZ	MP2	−65.6	7.19	6.41
	MP3	−81.6	7.06	6.27
	MP4	−88.4	7.02	6.24
	VB_V	−110.4	6.90	6.13
	expt[40]	−114.4	6.8	

[a] Interaction energy curves along three different radial trajectories (see text for details). [b] Counterpoise correction applied in all cases, with the exception of VB_V data.

In the case of the $He-CH_4$ complex, the global minimum VB/aug-cc-pVTZ interaction energy is significantly more attractive with respect to the MP4/aug-cc-pVTZ and experimental[40] data. Both MP4 and VB data indicate a larger PES anisotropy with respect to that predicted by Buck et al.[40]

The fundamental approximation of the present scheme is the inclusion of second-order interfragment correlation terms only. This gives a rationale to the fact that VB interaction energies are systematically larger than MP4, CCSD(T), and FCI results, when available. Quantitatively, this effect is not dramatic for weakly interacting systems such as the one detailed in the present work, and VB results are comparable in quality with respect to MP4 and CCSD(T) ones. Our approximation would probably be somewhat more severe in systems where intramonomer correlation terms give more marked contributions to the interaction energy such as, for example, systems for which a single configuration reference wave function is definitely not appropriate. In this regard, the definition of the proper strategy to include this terms in the final MO−VB wave function is currently under way in our laboratories.

Note Added after ASAP Posting. This article was released ASAP on 5/7/2002 before author corrections were included. The corrected article was posted on 5/8/2002.

References and Notes

(1) (a) Kestner, N. R. *J. Chem. Phys.* **1968**, *48*, 252. (b) van Lenthe, J. H.; van Duijneveldt-van de Rijdt, J. G. C. M.; van Duijneveldt, F. B. *Adv. Chem. Phys.* **1987**, *69*, 521.

(2) van Duijneveldt, F. B.; van Duijneveldt-van de Rijdt, J. G. C. M.; van Lenthe, J. H. *Chem. Rev.* **1994**, *94*, 1873.

(3) Boys, S. F.; Bernardi, F. *Mol Phys.* **1970**, *19*, 553.

(4) (a) Xantheas, S. S. *J. Chem. Phys.* **1996**, *104*, 8821. (b) Simon, S.; Duran, M.; Dannenberg, J. J. *J. Chem. Phys.* **1996**, *105*, 11024.

(5) Karlström, G.; Sadlej, A. J. *Theor. Chim. Acta* **1982**, *61*, 1.

(6) (a) Gianinetti, E.; Raimondi, M.; Tornaghi, E. *Int. J. Quantum Chem.* **1996**, *60*, 157. (b) Famulari, N.; Gianinetti, E.; Raimondi, M.; Sironi, M. *Int. J. Quantum Chem.* **1998**, *69*, 151.

(7) (a) Famulari, A.; Raimondi, M.; Sironi, M.; Gianinetti, E. *Chem. Phys.* **1998**, *232*, 275. (b) Famulari, A.; Moroni, F.; Sironi, M.; Gianinetti, E.; Raimondi, M. *J. Mol. Struct. (THEOCHEM)* **2000**, *529*, 209. (c) Moroni, F.; Famulari, A.; Raimondi, M. *J. Phys. Chem. A* **2001**, *105*, 1169.

(8) (a) Famulari, A.; Specchio, R.; Sironi, M.; Raimondi, M. *J. Chem. Phys.* **1998**, *108*, 3296. (b) Specchio, R.; Famulari, A.; Sironi, M.; Raimondi, M. *J. Chem. Phys.* **1999**, *111*, 6204. (c) Raimondi, M.; Famulari, A.; Specchio, R.; Sironi, M.; Moroni, F.; Gianinetti, E. *J. Mol. Struct. (THEOCHEM)* **2001**, *573*, 25.

(9) Specchio, R.; Famulari, A.; Martinazzo, R.; Raimondi, M. *J. Chem. Phys.* **2000**, *113*, 6724.

(10) (a) Liu, B.; McLean, A. D. *J. Chem. Phys.* **1980**, *72*, 3418. (b) Liu, B.; McLean, A. D. *J. Chem. Phys.* **1989**, *91*, 2348.

(11) (a) Raimondi, M.; Campion, W.; Karplus, M. *Mol. Phys.* **1977**, *34*, 1483. (b) Cooper, D. L.; Gerratt, J.; Raimondi, M. *Chem. Rev.* **1991**, *91*, 929.

(12) Hamza, A.; Vibok, A.; Halasz, G. J.; Mayer, I. *J. Mol. Struct. (THEOCHEM)* **2000**, *501*, 427.

(13) Chalasinski, G.; Szczesniak, M. M. *Chem. Rev.* **1994**, *94*, 1723.

(14) Schütz, M.; Brdarski, S.; Widmark, P.-O.; Lindh, R.; Karlström, G. *J. Chem. Phys.* **1997**, *107*, 4597.

(15) Nagata, T.; Takahashi, O.; Saito, K.; Iwata, S. *J. Chem. Phys.* **2001**, *115*, 3553.

(16) Dijkstra, F.; van Lenthe, J. H. *Chem. Phys. Lett.* **1999**, *310*, 553.

(17) Dijkstra, F.; van Lenthe, J. H. *J. Chem. Phys.* **2000**, *113*, 2100.

(18) Jeziorski, B.; Moszynski, R.; Szalewicz, K. *Chem. Rev.* **1994**, *94*, 1887.

(19) (a) Dunning, T. H., Jr. *J. Chem. Phys.* **1989**, *90*, 1007. (b) Kendall, R. A.; Dunning, T. H., Jr.; Harrison, R. J. *J. Chem. Phys*. **1992**, *96*, 6769. (c) Woon, D. E.; Dunning, T. H., Jr. *J. Chem. Phys.* **1994**, *100*, 2975.

(20) (a) Schmidt, M. W.; Baldridge, K. K.; Boatz, J. A.; Elbert, S. T.; Gordon, M. S.; Jensen, J.; Koseki, S.; Matsunaga, N.; Nguyen, K. A.; Su, S. J.; Windus, T. L.; Dupuis, M.; Montgomery, J. A. *J. Comput. Chem.* **1993**, *14*, 1347. (b) Granovsky, A. A. wwwhttp://classic.chem.msu.su/gran/gamess/index.html.

(21) Frisch, M. J.; Trucks, G. W.; Schlegel, H. B.; Scuseria, G. E.; Robb, M. A.; Cheeseman, J. R.; Zakrzewski, V. G.; Montgomery, J. A., Jr.; Stratmann, R. E.; Burant, J. C.; Dapprich, S.; Millam, J. M.; Daniels, A. D.; Kudin, K. N.; Strain, M. C.; Farkas, O.; Tomasi, J.; Barone, V.; Cossi, M.; Cammi, R.; Mennucci, B.; Pomelli, C.; Adamo, C.; Clifford, S.; Ochterski, J.; Petersson, G. A.; Ayala, P. Y.; Cui, Q.; Morokuma, K.; Malick, D. K.; Rabuck, A. D.; Raghavachari, K.; Foresman, J. B.; Cioslowski, J.; Ortiz, J. V.; Stefanov, B. B.; Liu, G.; Liashenko, A.; Piskorz, P.; Komaromi, I.; Gomperts, R.; Martin, R. L.; Fox, D. J.; Keith, T.; Al-Laham, M. A.; Peng, C. Y.; Nanayakkara, A.; Gonzalez, C.; Challacombe, M.; Gill, P. M. W.; Johnson, B. G.; Chen, W.; Wong, M. W.; Andres, J. L.; Head-Gordon, M.; Replogle, E. S.; Pople, J. A. *Gaussian 98*, revision A.9; Gaussian, Inc.: Pittsburgh, PA, 1998.

(22) Woon, D. E. *J. Chem. Phys.* **1994**, *100*, 2838.

(23) van Mourik, T.; Dunning Jr., T. H. *J. Chem. Phys.* **1999**, *111*, 9248.

(24) van Mourik, T.; Wilson, A. K.; Dunning, T. H. Jr. *Mol. Phys.* **1999**, *96*, 529.

(25) (a) Anderson, J. B.; Traynor, C. A.; Boghosian, B. M. *J. Chem. Phys.* **1993**, *99*, 345. (b) Anderson, J. B. *J. Chem. Phys.* **2001**, *115*, 4546.

(26) Korona, T.; Williams, H. L.; Bukowski, R.; Jeziorski, B.; Szalewicz, K. *J. Chem. Phys.* **1997**, *106*, 5109.

(27) Komasa, J.; Rychlewski, J. *Mol. Phys.* **1997**, *91*, 909.

(28) Burda, J. V.; Zahradník, R.; Hobza, P.; Urban, M. *Mol. Phys.* **1996**, *89*, 425.

(29) Aziz, R. A.; Janzen, A. R.; Moldover, M. R. *Phys. Rev. Lett.* **1995**, *74*, 1586.

(30) Janzen, A. R.; Aziz, R. A. *J. Chem. Phys.* **1997**, *107*, 914.

(31) Specchio, R.; Famulari, A.; Raimondi, M. *J. Mol. Struct. (THEOCHEM)* **2001**, *549*, 77.

(32) (a) Cohen, R. C.; Saykally, R. J. *J. Chem. Phys.* **1993**, *98*, 1007. (b) Tao, F.-M.; Klemperer, W. *J. Chem. Phys.* **1994**, *101*, 1129. (c) Bulski, M.; Wormer, P. E. S.; van der Avoird, A. *J. Chem. Phys.* **1991**, *94*, 8096.

(33) Green, S. *Astrophys. J. (Suppl.)* **1980**, *42*, 103.

(34) (a) Palma, A.; Green, S.; DeFrees, D. J.; McLean, A. D. *J. Chem. Phys.* **1988**, *89*, 1401. (b) Green, S.; DeFrees, D. J.; McLean, A. D. *J. Chem. Phys.* **1991**, *94*, 1346. (c) Maluendes, S.; McLean, A. D.; Green, S. *J. Chem. Phys.* **1992**, *96*, 8150. (d) Palma, A.; Green, S.; DeFrees, D. J.; McLean, A. D. *Astrophys. J. (Suppl.)* **1988**, *68*, 287. (e) Palma, A.; Green, S.; DeFrees, D. J.; McLean, A. D. *Astrophys. J. (Suppl.)* **1989**, *70*, 681.

(35) Tao, F.-M.; Li, Z.; Pan, Y.-K. *Chem. Phys. Lett*. **1996**, *255*, 179.

(36) Hodges, P. M.; Wheatley, R. J.; Harvey, A. H. *J. Chem. Phys.* **2002**, *116*, 1397.

(37) (a) Liebe, H. J.; Dillon, T. A. *J. Chem. Phys.* **1969**, *50*, 727. (b) Kasuga, T.; Kuze, H.; Shimizu, T. *J. Chem. Phys.* **1978**, *69*, 5195. (c) Goyette, T. M.; DeLucia, F. C. *J. Mol. Spectrosc.* **1990**, *143*, 346. (d) Godon, M.; Bauer, A. *Chem. Phys. Lett*. **1988**, *147*, 189.

(38) (a) Slankas, J. T.; Keil, M.; Kuppermann, A. *J. Chem. Phys.* **1979**, *70*, 1482. (b) Goldflam, R.; Green, S.; Kouri, D. J.; Monchick, L. *J. Chem. Phys.* **1978**, *69*, 598.

(39) Kukawska-Tarnawska, B.; Chalasinski, G.; Szczesniak, M. M. *J. Mol. Struct. (THEOCHEM)* **1993**, *297*, 313.

(40) Buck, U.; Kohl, K. H.; Kohlase, A.; Faubel, M.; Staemmler, V. *Mol. Phys.* **1985**, *55*, 1233.

(41) (a) Chapman, W. B.; Schiffman, A.; Hutson, J. M.; Nesbitt, D. J. *J. Chem. Phys.* **1996**, *105*, 3497. (b) Taylor, W. L. *J. Chem. Phys.* **1996**, *105*, 8333.

(42) Gao, D.; Chen, L.; Li, Z.; Tao, F.-M.; Pan, T.-K. *Chem. Phys. Lett.* **1997**, *277*, 483.

(43) Yin, D.; MacKerell, A. D., Jr. J. *Phys. Chem.* **1996**, *100*, 2588.